GEOPHYSICS, VOL. 67, NO. 3 (MAY-JUNE 2002); P. 921–927, 9 FIGS., 1 TABLE.
10.1190/1.1484534

Acoustic velocity of seismic-while-drilling (SWD) borehole guided waves

Flavio Poletto*, José M. Carcione*, Massimo Lovo*, and Francesco Miranda‡

ABSTRACT

Borehole guided waves, other than the extensional waves traveling through the drillstring, can be used as pilot signals to obtain seismic-while-drilling (SWD) seismograms and information about the drilling conditions. This occurs when there is no rotation of the drillstring while drilling and when the contacts between the drillpipe and the borehole wall preclude the propagation of the extensional wave. To obtain the velocity of the guided waves, we model the compressional-wave velocity of drilling mud with different compositions of low- and high-gravity solids, corresponding to a given drilling plan and taking into account the presence of formation cuttings and in-situ conditions. Then we compute the velocities of the tube wave (with and without casing) and the guided wave traveling in the mud inside the drillstring (pipe wave). The results indicate the pipe wave constitutes a reliable pilot signal in the absence of drillpipe rotation. This allows us to obtain a complete depth reverse vertical seismic profile.

INTRODUCTION

Drillstring guided waves contain information about drilling conditions (MacPherson et al., 1993; Hutchinson et al., 1995) and can be used to transmit data from the bit location to the surface. For instance, Rector and Marion (1991) and Miranda et al. (1996) investigate the potentials of the extensional waves traveling through the drillstring for while-drilling prediction ahead of the bit. Carcione and Poletto (2000a) solve the differential equations describing wave propagation through the drillstring. They compute waveforms of the extensional, torsional, and flexural waves by modeling the geometrical features of the coupling joints, including piezoelectric sources and sensors. These signals are used to correct the arrival time of the data acquired at the surface by a deployed seismic line. In the absence of axial waves, other guided modes can be used as pilot signals. This occurs when there is no rotation of the drillstring but rotation of the drill bit from the downhole motor (see Figure 1 and Poletto and Miranda, 1998).

The alternative pilot signals are the low-frequency Stoneley wave traveling between the mud and the formation (the so-called tube wave) and the wave traveling inside the drillpipe, filled with drilling mud (referred to here as the pipe wave). The velocity of these guided waves depends on the elastic properties of the surrounding formation, the borehole lateral dimensions, the drillstring diameters, and the body-wave velocity of the drilling mud. A typical seismic while drilling (SWD) experiment showing these conditions is displayed in Figure 2, where the dipping events were obtained with different pilot signals (Poletto and Miranda, 1998). The seismic traces belong to a correlated common receiver gather, obtained with (Figure 2a) and without (Figure 2b) drillstring rotation (the zero correlation time is 4 s). The data are displayed without pilot-delay correction. Figure 2a shows the correlation with the extensional wave recorded by an accelerometer located above the drillstring, and Figure 2b shows the correlation with a slower signal (interpreted later as a pipe wave) recorded by the same accelerometer.

The basic equations for synthetic acoustic logging in a fluid-filled borehole are given, for instance, in Cheng and Toksöz (1981), who investigate the dispersion curves of the Stoneley mode (tube waves). In their examples (hard formations), these waves show very little dispersion in the seismic frequency range, and both the phase and group velocities increase from about $0.9\,c_m$ at low frequencies (tube-wave limit) to about $0.96\,c_m$ at high frequencies, where c_m is the body-wave velocity in the drilling mud. The other factors affecting the tube-wave velocity are the compressional and shear velocities of the formation and the borehole lateral dimensions. In their analysis,

Manuscript received by the Editor February 22, 2001; revised manuscript received September 10, 2001.
*Istituto Nazionale di Oceanografia e di Geofisica Sperimentale—OGS, Borgo Grotta Gigante 42c, 34010 Sgonico, Trieste, Italy. E-mail: fpoletto@ogs.trieste.it; jcarcione@ogs.trieste.it; mlovo@ogs.trieste.it.
‡ENI-Agip Division, APSI Department, via dell'Unione Europea 3, 20097 S. Donato Milanese, Milano, Italy. E-mail: francesco.miranda@agip.it.

Cheng and Toksöz (1981) use a mud velocity $c_m = 1830$ m/s which, according to our calculations, is too high for actual drilling muds.

Lea and Kyllingstad (1996) consider the drillstring/borehole system, including the formation and the inner and outer drilling mud. They compute the velocities of the different wave modes by using a low-frequency approximation and conclude that wave coupling is most important between the fluid modes (inner and annular pressure waves). They assume a sound velocity of 1304 m/s for the inner and outer mud. Rama Rao and Vandiver (1999) analyze the acoustic properties of a water-filled borehole with pipes, calculating the axisymmetric propagation of the different modes for frequencies <1000 Hz and considering soft and hard formations. In the analysis, the authors use $c_m = 1558$ m/s, which is closer to our estimations than Cheng and Toksöz's (1981) velocity.

The sound velocity of drilling mud saturated with reservoir gas is modeled by Carcione and Poletto (2000b). They give the basic equations to calculate c_m for water- and oil-based drilling muds versus solid content and gas saturation, and for different temperature and pressure conditions. On the basis of these results, we compute the sound velocity of the drilling mud along the borehole, corresponding to a realistic drilling plan. The velocity of sound in drilling mud and the pipe dimensions

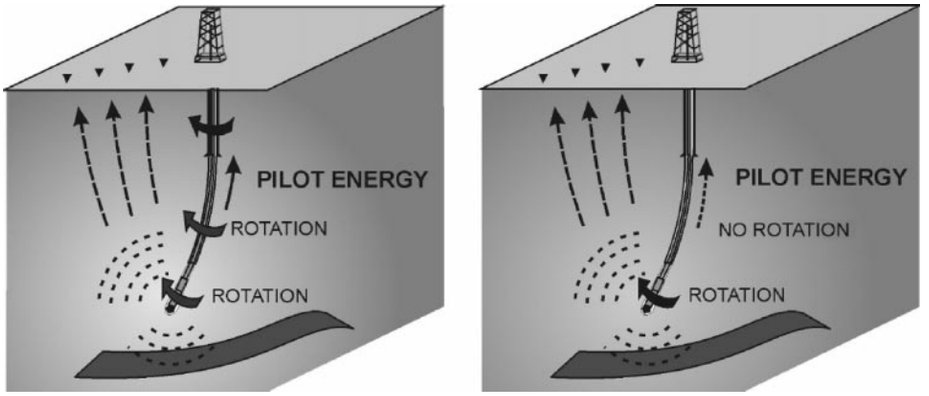

FIG. 1. Different drilling conditions with (left) and without (right) rotation of the drillstring. In the first case, the extensional wave traveling through the drillstring is used as pilot signal. In the second case, the possible alternative pilot signals are the Stoneley wave and the guided wave traveling in the drilling mud.

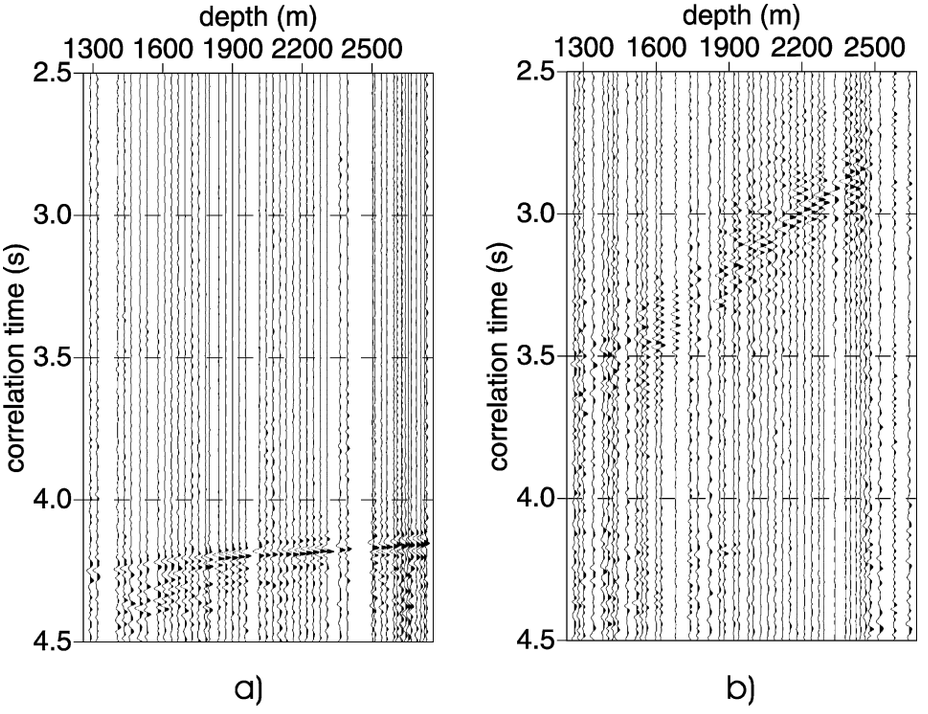

FIG. 2. SWD experiment showing (a) the correlation with the extensional wave recorded by an accelerometer located above the drillstring and (b) the correlation with a slower signal recorded by the same accelerometer. In the correlated data, a slower pilot signal appears at lower arrival times.

are the major factors affecting the velocity of the guided waves. These velocities are obtained from simple formulas, valid in the low-frequency approximation, i.e., when the wavelength of the signals is much longer than the borehole diameter. A sensitivity analysis provides further insight on the reliability of the results.

ACOUSTIC PROPERTIES OF DRILLING MUD

The composite density of drilling mud is the arithmetic average of the densities of the single constituents. Using the Einstein convention for repeated indices, the mud density is $\rho_m = \phi_i \rho_i$, where ϕ_i and ρ_i are the volume fraction and density of the low-gravity solids (bentonite or polymers) ($i = 1$), the high-gravity solids (barite) ($i = 2$), fluid (water) ($i = 3$), and cuttings ($i = 4$). By definition, $\phi_i \delta_{ij} = 1$, where δ_{ij} is Kronecker's delta. The volume fractions of bentonite and barite are provided by the mud logging company, or, alternatively, they can be calculated from the mud-weight profile versus depth, corresponding to the drilling plan (Carcione and Poletto, 2000b).

Wood's model is used to obtain the bulk modulus (Wood, 1955). The model averages the reciprocal of the single bulk moduli (isostress assumption). The composite bulk modulus is $K_m = (\phi_i / K_i)^{-1}$, where K_1, K_2, K_3, and K_4 are the bulk moduli of bentonite, barite, water, and cuttings, respectively. The mud-wave velocity is then given by

$$c_m = \sqrt{\frac{K_m}{\rho_m}}. \tag{1}$$

This velocity is generally lower than the wave velocity of the pure fluid (water in this case) because the increase in density from the presence of solids is not compensated by the increase in bulk modulus. Differentiating equation (1), we obtain

$$\frac{\delta c_m}{c_m} = \frac{1}{2}\left(\frac{\delta K_m}{K_m} - \frac{\delta \rho_m}{\rho_m}\right), \tag{2}$$

where δ denotes the increment (positive or negative) in the respective quantity.

Sensitivity analysis

Increasing the density by adding solids decreases the sound velocity, but an increase in bulk modulus increases the velocity. Hence, it is necessary to study how sound velocity varies when adding solids to the drilling mud. For simplicity, we assume a single additive solid with volume fraction $\phi_s = \phi_1$ or $\phi_s = \phi_2$. Differentiating the bulk modulus and the density with respect to the volume faction ϕ_s, we obtain

$$\frac{\delta c_m}{c_m} = \frac{1}{2}\left(\frac{K_s - K_f}{K_s - \phi_s(K_s - K_f)} - \frac{\rho_s - \rho_f}{\rho_f + \phi_s(\rho_s - \rho_f)}\right)\delta\phi_s, \tag{3}$$

where the subscripts s and f denote the solid and the fluid, respectively. The value $\phi_s = \phi^*$ at which the right side of equation (3) changes sign—and c_m has its minimum value—is

$$\phi^* = \frac{1}{2}\left(\frac{K_s}{K_s - K_f} - \frac{\rho_f}{\rho_s - \rho_f}\right). \tag{4}$$

Using the material properties given in Table 1, we obtain $\phi^* = 0.23$ for bentonite and $\phi^* = 0.37$ for barite, corresponding to $\rho_m = 1386$ kg/m^3 and $\rho_m = 2174$ kg/m^3. Figure 3 shows the sound velocity of drilling mud as a function of the volume fraction of (a) solids ϕ_s and (b) mud density ρ_m. The solid line corresponds to bentonite, the dashed line to barite. The sound velocity of drilling mud is lower than the sound velocity of water for realistic values of the volume fraction. In real applications barite is generally used in the drilling plans to obtain high values of mud weight. As can be seen, barite-saturated mud has a lower velocity than bentonite-saturated mud. Because of this, we expect sound velocities <1500 m/s.

The volume fraction of the cuttings in the outer mud is $\phi_4 = 84.45\, D^2\, \mathrm{ROP}/F$, where D is the diameter of the borehole (inches), ROP is the rate of penetration (m/hour), and

Table 1. Material properties.

Material	Density (kg/m^3)	Elastic properties (GPa)
Bentonite	2650	36$^+$
Barite	4200	55$^+$
Water	1000	2.25$^+$
Cuttings	2000	23$^+$
Pipe	7840	206* 0.29†

$^+$Bulk modulus
*Young modulus
†Poisson's ratio.

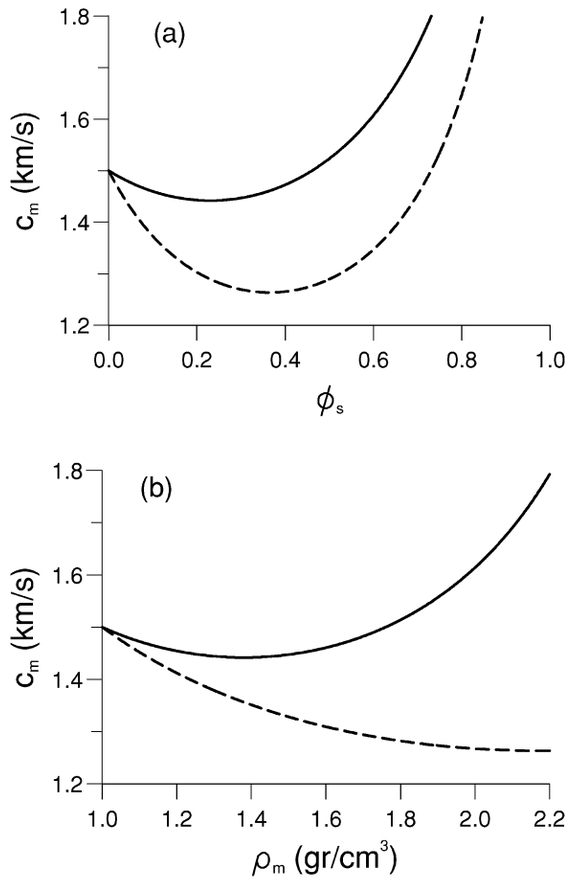

FIG. 3. Sound velocity of drilling mud as a function of the volume fraction of (a) solid ϕ_s and (b) mud density ρ_m. The solid line corresponds to bentonite, the dashed line to barite.

F is the pump flow rate of the mud (liters/min) (Gabolde and Nguyen, 1999, p. G10). This volume fraction becomes significant for high rates of penetration (ROP > 30 m/hour) and large bit diameters, since the amount of cuttings increases the density of the mud and affects its sound velocity.

VELOCITIES OF GUIDED WAVES

The velocity of the pipe waves is given by

$$c_p = \left[\rho_m\left(\frac{1}{K_m}+\frac{1}{M}\right)\right]^{-1/2}, \tag{5}$$

where

$$M = \frac{E(a^2-b^2)}{2[(1+\nu)a^2+(1-\nu)b^2]}, \tag{6}$$

a and b are the outer and inner radii of the pipe, and E and ν are the Young modulus and Poisson ratio of the pipe (White, 1965, p. 150). This approximation holds at low frequencies and assumes that the outer medium is a vacuum.

On the other hand, the velocity of the Stoneley mode in the absence of a drillstring is obtained from equation (5) by taking $M=\mu$, where μ is the shear modulus of the formation:

$$c_S = \left[\rho_m\left(\frac{1}{K_m}+\frac{1}{\mu}\right)\right]^{-1/2}. \tag{7}$$

The presence of casing in the upper sections of the borehole must be considered. If we include the steel casing, the tube-wave velocity is

$$c_T = \left[\rho_m\left(\frac{1}{K_m}+\frac{1}{\mu+(Eh/2b')}\right)\right]^{-1/2}, \tag{8}$$

where a' and b' are the outer and inner radii of the casing and $h=a'-b'$ (White, 1965, p. 155). Equation (8) assumes there is no mud between the casing and the formation but that the corresponding interface is lubricated. Note that we do not consider the borehole in the presence of drillstring.

The accuracy of the low-frequency approximations (5), (7), and (8) have been verified by comparison with the exact expressions provided by Rama Rao and Vandiver (1999) and Lea and Kyllingstad (1996). Rama Rao and Vandiver (1999) consider hard and soft formations and show that, at low frequency, the difference between the approximated and the exact pipe-wave velocities is 0.07% and 0.35%, respectively. The differences for the Stoneley mode are 3.5% and 7% for the hard and soft formations, respectively. On the other hand, the differences for the pipe and tube waves compared to the values obtained by Lea and Kyllingstad (1996) for a soft formation are 0.04% and 6%, respectively. Unlike the tube (Stoneley) waves, the pipe waves are not very sensitive to the properties of the formation.

Sensitivity analysis

Let us analyze the sensitivity of the pipe-wave velocity in terms of the bulk modulus and density of the drilling mud and in terms of modulus M. We consider the variation of M for new- and worn-pipe conditions. Differentiating equation (5), we obtain

$$\frac{\delta c_p}{c_p} = \frac{1}{2}\left[\left(\frac{c_p}{c_m}\right)^2\frac{\delta K_m}{K_m}-\frac{\delta\rho_m}{\rho_m}+\left(\frac{\rho_m c_p^2}{M}\right)\frac{\delta M}{M}\right]. \tag{9}$$

Let us define the relative-wear coefficient

$$\delta_w = \frac{\delta a-\delta b}{a-b}. \tag{10}$$

If $\delta a=-\delta b$, $a+b$ is constant. Moreover, if $0\le\delta_w\le 0.2$, the denominator in equation (6) is nearly constant. Hence, we have

$$\frac{\delta M}{M} \cong \delta_w. \tag{11}$$

Assuming one saturating solid, we can recast equation (9) in terms of the volume fraction of the solid. Using equation (11), we obtain

$$\frac{\delta c_p}{c_p} = \frac{1}{2}\left\{\left[\left(\frac{c_p}{c_m}\right)^2\frac{K_s-K_f}{K_s-\phi_s(K_s-K_f)} - \frac{\rho_s-\rho_f}{\rho_f+\phi_s(\rho_s-\rho_f)}\right]\delta\phi_s+\left(\frac{\rho_m c_p^2}{M}\right)\delta_w\right\}. \tag{12}$$

EXAMPLE

The well under investigation is located in southern Italy (Basilicata province), where the reservoir rock is the Apula Formation, constituted by limestones. The casing program and average mud density versus drill-bit depth is shown in Figure 4, and the material properties of the different media are given in Table 1. We assume, for simplicity, an average value of the volume fraction of cuttings versus depth, with

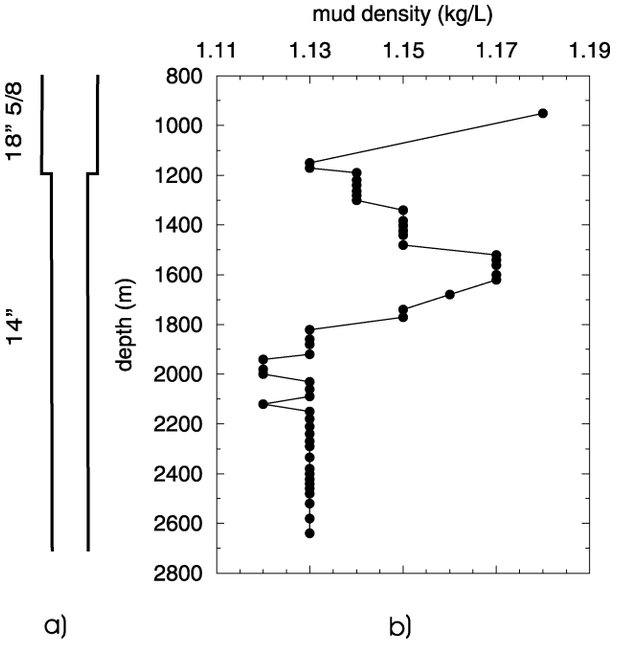

FIG. 4. (a) Casing program and (b) average mud density versus drill-bit depth. The proportion of fluids (water) and bentonite versus depth are provided by the mud logging company.

ROP = 8 m/hour, $F = 4000$ liters/min, and $D = 0.3$ m. This approximation should be modified to consider varying rates of penetration and bit radii versus depth. However, the influence of the fraction of cuttings is not very important for low and moderate ROP.

Since the average mud weight varies as a function of drill-bit depth, the sound speed down to each depth varies as a function of drill-bit depth. At any particular depth, the sound speed of any mode will then be a function of the average density and the drillstring hardware at that depth. Both will change as the drilling progresses. Figure 5 shows the velocities of the different wave modes as a function of depth. They have been calculated by using the drill-pipe, tool-joint, and bottom-hole-assembly (BHA) composition, dimension, and length, considering worn and new pipes. The calculations do not take into account pressure and temperature effects. The drillstring radii are $a = 0.063$ m and $b = 0.054$ m for the pipes and $a = 0.084$ m and $b = 0.033$ for the tool joints. Their lengths are 9.2 and 0.5 m, respectively. For the worn pipes, we assume a 20% reduction of the pipe thickness. The outer and inner radii of the casing are $a' = 0.178$ m and $b' = 0.163$ m, and the formation shear modulus is calculated as $\mu = 800\, v_P^2$, where v_P is the P-wave velocity obtained from the sonic log, given in meters per second. The highest velocity in Figure 5 is the sound velocity of the drilling mud. The variations are mainly because of the changes in drilling-mud density. The mean-squared errors between the modeled and experimental velocities are shown in Figure 6. This indicates that the slower pilot signals recorded by the accelerometer are, with good probability, pipe waves. The minimum error is obtained for worn pipes (premium class and 20% thickness reduction). The comparison between the picked traveltimes (dots) and the traveltimes calculated with the theoretical pipe-wave velocity (solid line) is shown in Figure 7. The agreement is excellent. The complete seismogram is represented in Figure 8b. The same event, showing different traveltimes in Figure 8a, has been corrected to the position associated with the extensional-wave pilot signal by using the calculated pipe-wave velocity in the absence of drillstring rotation (Poletto and Miranda, 1998). Finally, Figure 9 shows the

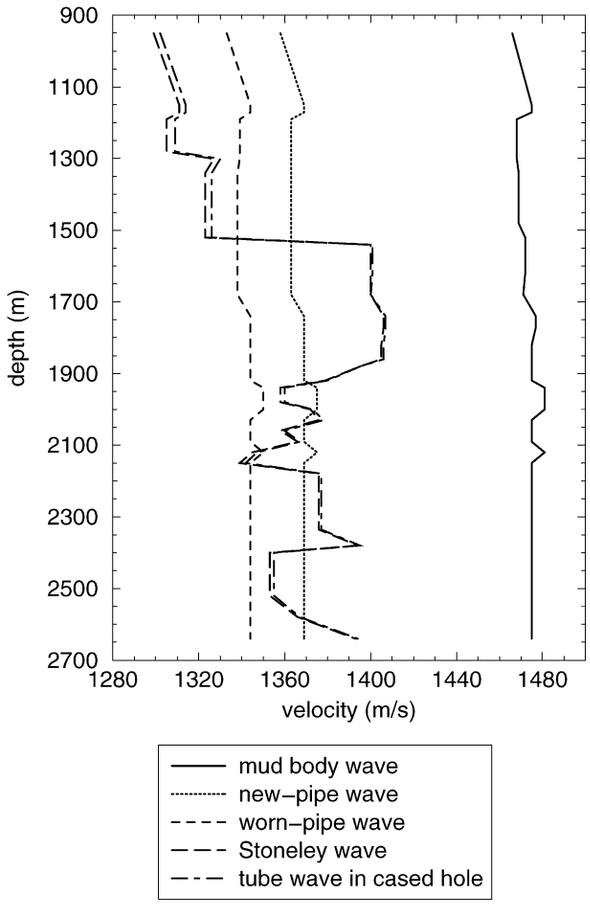

FIG. 5. Velocities of the different wave modes as a function of depth: mud body wave [equation (1)], worn-pipe and new-pipe waves [equation (5)], Stoneley wave [equation (7)], and tube wave in a cased hole [equation (8)].

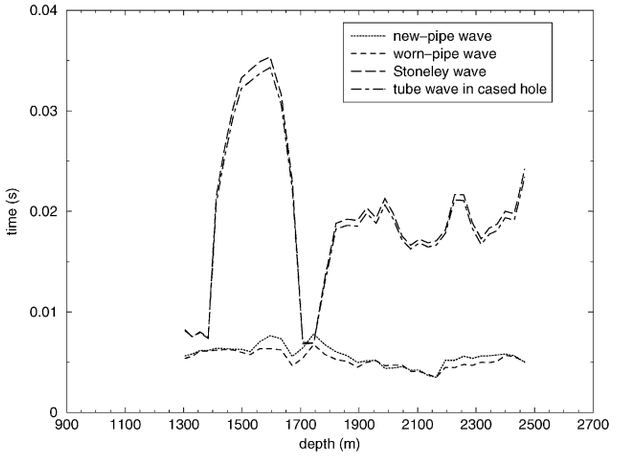

FIG. 6. Mean-squared errors between the calculated and experimental velocities. The experimental velocity corresponds to the event shown in Figure 2b.

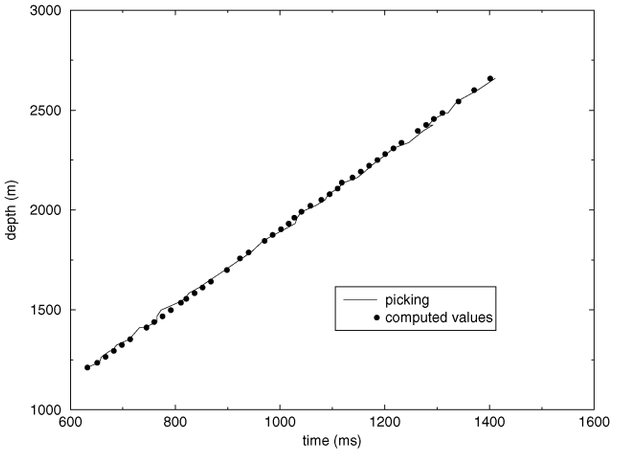

FIG. 7. Comparison between the picked traveltimes (dots) and the traveltimes calculated with the computed pipe-wave velocity (solid line).

two-way traveltime SWD seismograms, where the reflections events can be appreciated. Figure 9a includes all the traces, but the pipe-wave pilot signal is not used. In Figure 9b only the traces obtained with drillstring rotation are considered. Figure 9c includes all of the traces, processed with both pilot signals. The improvement obtained by using the pipe waves can be seen in the continuity of the events.

Equation (12) allows us to perform a sensitivity analysis of the pipe-wave velocity [equation (5)] versus solid fraction and worn conditions. Assuming $\phi_s = 0.09$, $\rho_m = 1148\ \mathrm{kg/m^3}$ (see Figure 4), $a = 0.063$ m, and $b = 0.054$ m, we obtain $c_m = 1463$ m/s and $c_p = 1356$ m/s (the tool joints have been neglected in this calculation). The bulk-modulus and density terms in the right side of equation (12) have opposite signs. If $\delta\phi_s = 0.01$,

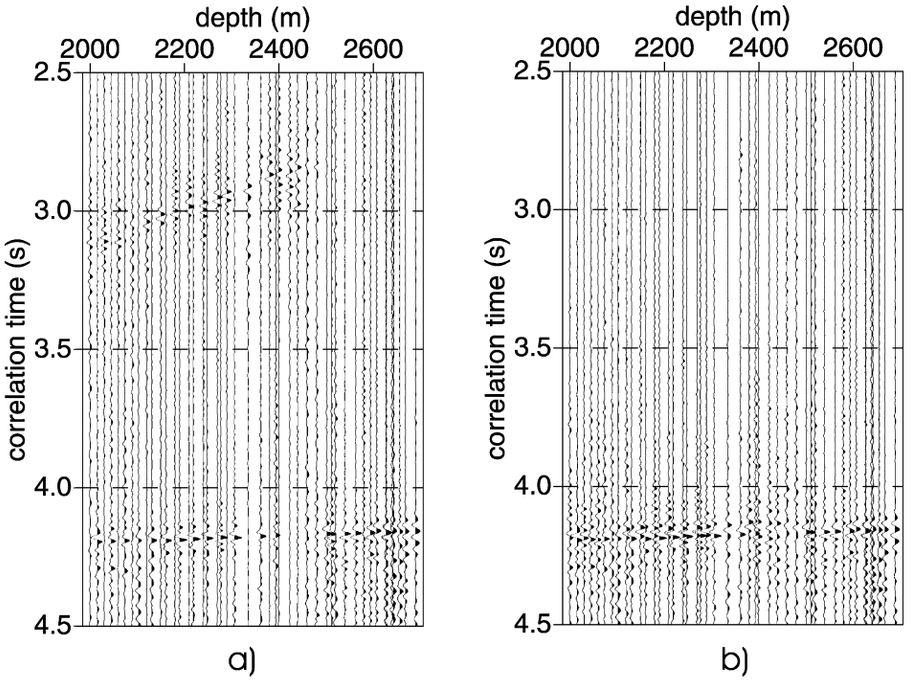

FIG. 8. Uncorrected (a) and corrected (b) seismograms, using both pilot signals, the extensional wave (with drillstring rotation), and the pipe wave (without drillstring rotation). In (a), we can appreciate the same event with different traveltimes.

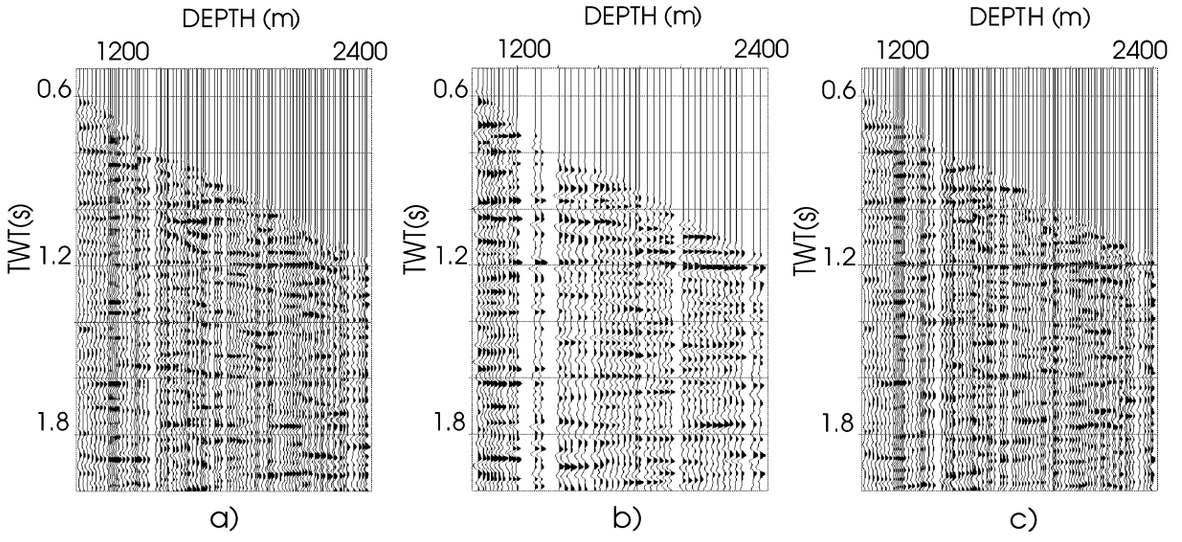

FIG. 9. Two-way traveltime SWD seismograms. (a) All of the traces (with and without drillstring rotation), processed with the axial wave as the pilot signal. (b) Only the traces obtained with drillstring rotation. (c) All of the traces processed with both the axial wave and the pipe wave.

$\delta c_p = -3.8$ m/s and $\delta c_p/c_p = -0.0028$, of which 0.0044 corresponds to the bulk-modulus term and -0.0072 is from the density term. Let us now consider the third term in the right side of equation (12). A relative wear $\delta_w = -0.05$ implies $\delta c_p = -4.8$ m/s and $\delta c_p/c_p = -0.0035$. Hence, the total decrease in the pipe-wave velocity is 8.6 m/s, in agreement with the variations observed in Figure 5.

CONCLUSIONS

We modeled the wave velocity of the different borehole modes observed in SWD seismograms to investigate their use as pilot signals. The extensional wave is difficult to detect when there is no rotation of the drillstring, and this precludes its use as a pilot signal. An alternative solution is given by the wave traveling through the drilling mud inside the pipes. This wave is weaker than the extensional wave but allows us to obtain a complete SWD seismogram under different drilling conditions.

ACKNOWLEDGMENTS

The authors thank ENI-Agip for the permission to publish this article.

REFERENCES

Carcione, J. M., and Poletto, F., 2000a, Simulation of stress waves in attenuating drill strings, including piezoelectric sources and sensors: J. Acoust. Soc. Am., **108**, No. 1, 53–64.

——— 2000b, Sound velocity of drilling mud saturated with reservoir gas: Geophysics, **65**, 646–651.

Cheng, C. H., and Toksöz, M. N., 1981, Elastic wave propagation in fluid-filled boreholes and synthetic acoustic logs: Geophysics, **46**, 1042–1053.

Gabolde, G., and Nguyen, J.-P., 1999, Drilling data handbook: Éditions Technip.

Hutchinson, M., Dubinsky, V., and Henneuse, H., 1995, An MWD downhole assistant driller: SPE paper 30523.

Lea, S.-H., and Kyllingstad, A., 1996, Propagation of coupled pressure waves in borehole with drillstring: SPE paper 37156.

MacPherson, J. D., Mason, J. S., and Kingman, J. E. E., 1993, Surface measurement and analysis of drill string vibrations while drilling: SPE/IADC paper 25777.

Miranda, F., Aleotti, L., Abramo, F., Poletto, F., Craglietto, A., Persoglia, S., and Rocca, F., 1996, Impact of seismic while drilling technique on exploration wells: First Break, **14**, 55–68.

Poletto, F., and Miranda, F., 1998, Seismic while drilling use of pilot signals with downhole motor drilling: 68th Ann. Internat. Mtg., Soc. Expl. Geophys., Expanded Abstracts, 147–150.

Rama Rao, V. N., and Vandiver, J. K., 1999, Acoustics of fluid filled boreholes with pipe: Guided propagation and radiation: J. Acoust. Soc. Am., **105**, No. 6, 3057–3066.

Rector, J. W., III, and Marion, B. P., 1991, The use of drill-bit energy as a downhole seismic source: Geophysics, **56**, 628–634.

White, J. E., 1965, Seismic waves: Radiation, transmission, and attenuation: McGraw-Hill Book Co.

Wood, A. B., 1955, A texbook of sound: Macmillan Co.